Free Radical Biology and Medicine 117 (2018) 132–144

Contents lists available at ScienceDirect

Free Radical Biology and Medicine

journal homepage: www.elsevier.com/locate/freeradbiomed

Original article

# Reactive oxygen species released from astrocytes treated with amyloid beta oligomers elicit neuronal calcium signals that decrease phospho-Ser727-STAT3 nuclear content

Yorka Muñoz[a], Andrea C. Paula-Lima[b,*], Marco T. Núñez[a,**]

[a] Department of Biology, Faculty of Sciences,Universidad de Chile, Santiago, Chile
[b] Institute for Research in Dental Sciences, Faculty of Dentistry, Universidad de Chile, Santiago, Chile

ARTICLE INFO

*Keywords:*
Neurons
STAT3
Astrocytes
Amyloid beta oligomers
Reactive oxygen species
Calcium

ABSTRACT

The transcription factor STAT3 has a crucial role in the development and maintenance of the nervous system. In this work, we treated astrocytes with oligomers of the amyloid beta peptide (AβOs), which display potent synaptotoxic activity, and studied the effects of mediators released by AβOs-treated astrocytes on the nuclear location of neuronal serine-727-phosphorylated STAT3 (pSerSTAT3). Treatment of mixed neuron-astrocyte cultures with 0.5 μM AβOs induced in neurons a significant decrease of nuclear pSerSTAT3, but not of phosphotyrosine-705 STAT3, the other form of STAT3 phosphorylation. This decrease did not occur in astrocyte-poor neuronal cultures revealing a pivotal role for astrocytes in this response. To test if mediators released by astrocytes in response to AβOs induce pSerSTAT3 nuclear depletion, we used conditioned medium derived from AβOs-treated astrocyte cultures. Treatment of astrocyte-poor neuronal cultures with this medium caused pSerSTAT3 nuclear depletion but did not modify overall STAT3 levels. Extracellular catalase prevented the pSerSTAT3 nuclear depletion caused by astrocyte-conditioned medium, indicating that reactive oxygen species (ROS) mediate this response. This conditioned medium also increased neuronal oxidative tone, leading to a ryanodine-sensitive intracellular calcium signal that proved to be essential for pSerSTAT3 nuclear depletion. In addition, this depletion decreased BCL2 and Survivin transcription and significantly increased BAX/BCL2 ratio. This is the first description that ROS generated by AβOs-treated astrocytes and neuronal calcium signals jointly regulate pSerSTAT3 nuclear distribution in neurons. We propose that astrocytes release ROS in response to AβOs, which by increasing neuronal oxidative tone, generate calcium signals that cause pSerSTAT3 nuclear depletion and loss of STAT3 protective transcriptional activity.

## 1. Introduction

Signal Transducers and Activators of Transcription (STATs) are latent factors that following activation translocate to the cell nucleus where they promote transcription of target genes [13,24,74]. The STAT3 proteins include the unphosphorylated form (STAT3) as well as the forms phosphorylated at Tyr705 (pTyrSTAT3) or Ser727 (pSerSTAT3) [74]. Under basal conditions, STAT3 is present in the cytoplasm [13,76], where it is inactive at the transcriptional level. Pro-inflammatory cytokines, mainly from the IL-6 family, induce the phosphorylation of STAT3 at its tyrosine 705 residue via activation of JAK kinases [68]. Phosphorylation at tyrosine 705 causes STAT3 dimerization and translocation to the nucleus, where it binds to specific DNA sequences and induces the upregulation of neuroprotective and neurotrophic genes [13,17,24,74]. STAT3 has been proposed as a critical transcriptional factor for the development and maintenance of the nervous system [15,62], and has been involved as well in immune responses, inflammation, survival and neuronal regeneration [7,27].

In addition to pTyrSTAT3, pSerSTAT3 is required for full STAT3 transcriptional activity [14,68]. Mice expressing STAT3 with serine 727 replaced by alanine have 50% of the transcriptional response in their fibroblasts compared to wild-type cells, and a decreased number of

*Abbreviations:* ACM, astrocyte conditions medium; AraC, 1-*b*-D-arabinofuranosylcytosine; AβOs, amyloid beta oligomers; BAPTA, 1,2-bis(o-aminophenoxy)ethane-N,N,N′,N′-tetraacetic acid; CAT, Catalase; DAPI, 4',6-diamidino-2-phenylindole; , DMTU, Dimethylthiourea; iNOS, inducible Nitric oxide synthase; Jak2, Janus kinase 2; MCI-186, 3-Methyl-1-phenyl-2-pyrazolin-5-one; NGF, nerve growth factor; ROI, region of interest; ROS, reactive oxygen species; SOD, Superoxide dismutase; STAT, Signal Transducers and Activators of Transcription; tBHP, tert-Butyl-hydroperoxide; Tempol, 1-oxyl-2,2,6,6-tetramethyl-4-hydroxypiperidine

* Corresponding author.
** Correspondence to: Biology Department, Faculty of Sciences, Universidad de Chile, Las Palmeras 3425, Santiago 7800024, Chile.
*E-mail addresses:* andreacpaulalima@u.uchile.cl (A.C. Paula-Lima), mnunez@uchile.cl (M.T. Núñez).

https://doi.org/10.1016/j.freeradbiomed.2018.01.006
Received 23 June 2017; Received in revised form 19 December 2017; Accepted 4 January 2018
Available online 05 January 2018
0891-5849/ 

thymocytes associated with increased apoptosis [55]. Gene expression analysis by microarray assays revealed that more than a thousand mRNAs have their levels altered in response to increased expression of wild type STAT3 or of the mutant form Tyr705PheSTAT3 [72]. Similarly, an antibody that binds specifically to the pTyr705 site blocks both pTyrSTAT3 nuclear accumulation and the expression of acute phase response proteins induced by interleukin-6; however, this antibody does not block the downstream effects of pSerSTAT3 or of the unphosphorylated STAT3 protein [33], indicating that pSerSTAT3 exhibits transcriptional activity independent of pTyrSTAT3. In addition, expression of the mutant Tyr705PheSTAT3 or of wild-type STAT3 in STAT3-null cells revealed that STAT3 transcriptional activity is independent of pTyrSTAT3 [72]. STAT3 phosphorylation at the serine 727 residue enhances STAT3 transcriptional activity [68], but does not seem to enhance STAT3 DNA binding activity [67]. Altogether, these observations point to an undetermined function of pSerSTAT3 that leads to the enhancement of STAT3 transcriptional activity.

Several lines of evidence suggest that cellular redox changes modify STAT3 activity. In non-neuronal cells ROS upregulate STAT3 tyrosine phosphorylation and binding activity [10,41,49,58]. Other reports indicate that STAT3 is a transcriptional factor susceptible to oxidative stress [36,37,41], and that hydrogen peroxide treatment induces STAT3 oligomerization through the formation of disulfide bonds [36,37,60]. In addition, oxidation of conserved cysteines in the STAT3 DNA-binding domain hinders its transcriptional activity [9,36]. Moreover, mild oxidative stress induces S-glutathionylation of STAT3, decreasing its nuclear accumulation and impairing the expression of target genes [8,71].

In response to ROS, STAT3 plays a critical role in brain development and promotes the survival of adult neurons under normal conditions [42]. Yet, STAT3 also plays a pivotal role under pathological conditions [30,53]. A previous study proposed that amyloid-beta (Aβ) peptide aggregates, known as the causative agents in Alzheimer´s disease, produce memory impairment by disturbing the JAK2/STAT3 axis in hippocampal neurons [12]. A decrease in either the expression or the activation of STAT3 markedly attenuated Aβ-induced neuronal apoptosis, suggesting that STAT3 activation contributes to neuronal death following exposure to Aβ [66]. In addition, it has been proposed that STAT3 acetylation and phosphorylation are involved in the responsiveness of microglia to the β−amyloid peptide [18]. A recent report showed that apolipoprotein E deletion in astrocytes, by specifically inhibiting TGF-α/Smad2/STAT3 signaling, ameliorates the spatial learning and memory deficits observed in APP/PS1 mice, a rodent Alzheimer's disease (AD) model [75]. Moreover, the pro-inflammatory effect of Aβ on macrophages has been related to STAT1 and STAT3 inactivation, and the JAK/STAT3 pathway was proposed as a common inducer of astrocyte reactivity in AD and Huntington diseases [6].

Astrocytes are essential for normal neuronal function. They participate in the homeostasis of fluids and neurotransmitters, and provide energy substrates to neurons, among other functions [52,54,57]. In addition, activated astrocytes secrete cytokines, such as IL-6, TNFα and IL-1α [11,43,69], which act directly on neurons, astrocytes and microglia amplifying inflammatory signals and inducing toxic effects on neurons [22]. Cytokines are known to contribute to the progression and severity of AD; they increase cell death *in vitro and in vivo* as well as in tissue models from AD patients. Moreover, the reactivity of astrocytes to noxious stimuli such as the soluble oligomers of the amyloid beta peptide (AβOs), the most synaptotoxic Aβ aggregates, has linked them to the degeneration of adjacent neurons in AD [11,43,69]. Treatment of astrocytes with AβOs produces mitochondrial dysfunction, activation of astrocytic NOX and induction of iNOS [1,2,69].

Here, we hypothesized that treatment of astrocytes with AβOs is likely to mediate the degeneration of adjacent neurons through inhibitory modulation of transcription factors involved in neuronal survival. Accordingly, we investigated the interplay between AβOs, astrocytes and neurons, and if AβOs-treated astrocytes contribute to neuronal pathology by affecting the survival of adjacent neurons at early stages. The present results highlight pSerSTAT3 as a critical transcription factor for the expression of genes implicated in neuronal cell survival, whose activity is inhibited by AβOs-treated astrocytes.

## 2. Materials and methods

Aβ 1–42 peptide was purchased from Bachem Inc. Hexafluoro-2-propanol (HFIP) and FluorSave Reagent were from Merck, dimethyl sulfoxide (DMSO), Superoxide dismutase (SOD), Catalase (CAT), Hemoglobin, CNBr-activated Sepharose matrix and mouse Anti-β actin were obtained from Sigma-Aldrich. Total RNA columns were obtained from Omega Bio-Tek Inc. MLV Reverse transcriptase enzyme was from Fisher Scientific-Invitrogen and KAPA SYBR® FAST Universal qPCR kit was from KAPA Biosystems. Nerve growth Factor (NFG), Neurobasal medium, HBSS, Glutamax, B27 supplement, Minimal essential medium (MEM), Dulbecco minimal essential medium (DMEM), Horse serum and Lipofectamine 2000 were from Fisher Scientific-Invitrogen. Fetal bovine serum (FBS) was from Biological Industries. Rabbit anti-phospho serine727-STAT3, mouse anti-phospho tyrosine705-STAT3, mouse anti-STAT3 and mouse anti-GFAP were from Cell Signaling Technology. Rabbit anti-histone H1 antibody (ab61177) and mouse anti-actin antibody (A5441) were from Abcam and Sigma, respectively. Chicken anti-βII-tubulin was purchased from Aves Lab. Goat Alexa Fluor® 488 anti-rabbit, Goat Alexa Fluor® 488 anti-mouse, Goat Alexa Fluor® 546 anti-chicken, Goat Alexa Fluor® 633 anti-mouse, Fluo4-AM, Alexa Fluor® 488 C5 Maleimide, Alexa Fluor® 555 C5 Maleimide and SuperSignal chemiluminescence assay kit were obtained from Thermo Fisher Scientific-Invitrogen. The HyperCyto plasmid was from Evrogen. BAPTA was purchased from Molecular Probes.

### 2.1. Preparation of AβOs

The Aβ1–42 peptide, prepared as a dried hexafluore-2-propanol film, was stored at −80 °C for up to 4 months. Before use, this peptide film was dissolved with sufficient sterile DMSO to make a 5 mM stock solution. To prepare AβOs by using standard methods [34,47], the 5 mM peptide solution was subsequently diluted to 100 μM with cold phosphate-buffered saline (PBS), aged overnight at 4 °C without agitation and centrifuged at 14,000 g for 10 min at 4 °C to remove insoluble aggregates (protofibrils and fibrils). The supernatant containing soluble AβOs was transferred to clean tubes and stored at 4 °C. The oligomeric nature of the aggregates in fresh preparations was confirmed by Western blot analysis and transmission electron microscopy as described previously [47]. Only fresh AβOs preparations (up to 2 days-old) were used. Fresh AβO preparations showed abundant oligomers with the classic spherical morphology previously described [35]; Aβ fibrils were not observed in these fresh AβO preparations.

### 2.2. Primary cultures

The Ethics Committee of the Faculty of Science, Universidad de Chile, approved the bioethical protocol used in this study. All procedures were performed in accordance with the Guideline for the Care and Use of Laboratory Animals from the National Institutes of Health, USA. Animals were housed with food and water *ad libitum*. Animals were euthanized under deep anesthesia to avoid animal suffering at each stage of the experiments.

Primary hippocampal cultures were prepared from 19-day-old embryos obtained from pregnant Sprague–Dawley rats, as previously described [31]. In brief, brains were removed and placed in a dish containing Hank's-HEPES solution. Meningeal membranes were removed, hippocampi were dissected and 0.5%, trypsin was added for 20 min. After this, cells were dissociated in Hank's-HEPES solution and suspended in MEM medium supplemented with 10% horse serum. Dissociated cells were plated on polylysine-coated plates and incubated for 1 h. After this, MEM was replaced by Neurobasal medium

supplemented with B-27. Cells were cultured for 7–8 days in vitro (7–8 DIV) at 37 °C in a humidified 5% $CO_2$ atmosphere. These cultures were substantially enriched in neurons, identified with a neuronal anti-βIII-tubulin antibody, with a glial content ~ 12% as revealed by immunocytochemistry staining for glial fibrillary acidic protein (Supplementary Figure 1). For the purpose of this work, the neuron-12% astrocyte culture is referred as astrocyte-rich neuronal culture. Astrocyte-poor neuronal cultures were obtained after 1-*b*-D-arabinofuranosylcytosine (AraC) treatment. Twenty-four hours after plating, 1.5 μM AraC was added to prevent glial proliferation; the resulting cultures showed 4% glial content (Supplementary Figure 1).

Rat cortical astrocytes were obtained as described [64] with modifications. Briefly, cerebral cortex from 1- to 3-day-old Sprague–Dawley either male or female rat pups were dissected in Hank's-buffered salt solution and digested using 0.25% trypsin supplemented with 0.5 mg/mL DNase I. The mixed astrocyte/microglia cultures were incubated in Dulbecco minimum essential medium containing 10% fetal bovine serum (FBS). After 13 days in culture, cells were vigorously stirred on a shaker at 300 rpm for 72 h to detach microglial cells. After shaking, astrocytes were trypsinized, replated into 35-mm plates or P60 plates, and grown until confluence prior to use (Supplementary Figure 2).

### 2.3. Astrocyte-conditioned medium (ACM)

Conditioned media from astrocytes cultured in Neurobasal supplemented with B27 was obtained after 24 h of treatment with 0.5 μM AβOs. This conditioned medium was used fresh. In all experiments using ACM, astrocytes-poor neuronal cultures were incubated for 24 h with this medium prior to evaluation of the parameters under study. Control astrocyte medium was obtained from astrocytes incubated for 24 h in culture medium without added AβOs.

### 2.4. Immunocytochemistry

Hippocampal neuron-astrocyte mixed cultures or astrocyte-poor neuronal cultures (7 DIV) were fixed with 4% formaldehyde/ 4% sucrose in PBS buffer for 5 min. Then, this solution was replaced by 4% paraformaldehyde/ 4% sucrose and cells were incubated for an additional 10 min, rinsed with PBS, incubated with 0.1% Triton X-100 in PBS for 30 min and blocked with 10% BSA-PBS for 1 h. Cells were immunolabeled by overnight incubation at 4 °C with different antibodies diluted in 3% BSA-PBS. Rabbit anti-pSer727STAT3 (1:50), chicken anti-βIII-tubulin (1:1000), mouse anti-GFAP (1:500), mouse anti-pTyr705STAT3 (1:100) and mouse anti-STAT3 (1:100) antibodies were used. Cells were then rinsed with PBS and incubated for 2 h at room temperature with goat Alexa Fluor 488 anti-rabbit, goat Alexa Fluor 633 anti-mouse, goat Alexa 488 anti-mouse or goat Alexa Fluor 546 anti-chicken as secondary antibodies (1:300 in 3% BSA in PBS). DAPI (1: 10,000) was used to stain nuclei. Coverslips were mounted in Fluor Save (Merck) and cells were visualized on a Zeiss LSM 710 confocal microscope system (Carl Zeiss Microscopy GmbH: Jena, Germany) using a 63 × oil objective. Images were digitally acquired with the ZEN software (Zeiss). The ImageJ software program (National Institutes of Health, Baltimore, MD) was used for image analysis and generation of zeta projections from five to seven stacks (0.4-mm thickness each one). Large fields containing 30 cells were imaged. Using the ROI manager tool, total neuronal areas were selected for the βIII-tubulin channel and the integrated density of pSerSTAT3 was measured in this channel using the Overlay tool, which transferred ROIs from one channel to another in the same position. After that, nuclear areas were selected through the DAPI channel and these areas were transferred to pSerSTAT3 channel. Cytoplasmic intensity was calculated as the difference between the total pSerSTAT3 intensity and the pSerSTAT3 nuclear intensity. The distribution is presented as a ratio between nuclear and cytoplasmic fluorescence of pSerSTAT3. All data are normalized respect to Control.

### 2.5. Preparation of nuclear and cytoplasmic extracts

Nuclear and cytosolic extracts were prepared as described previously [21]. In brief, cultured cells were washed with cold PBS and 100 μL of cold buffer A (10 mM HEPES, pH 7.9, 1.5 mM $MgCl_2$, 10 mM KCl, 0.5 mM DTT, 0.05% Nonidet P-40, plus serine protease inhibitors: 5 mM $Na_3VO_4$, 40 mM NaF, 10 mM $Na_4P_2O_7$) was added and incubated for 20 min in ice. The homogenate was centrifuged at 900 g for 10 min. The supernatant corresponds to the cytoplasmic fraction. The pellet was washed three times with 100 μL of buffer A. The nuclear pellet was resuspended in 50 μL of hypertonic cold buffer B (5 mM HEPES, pH 7.9, 1.5 mM $MgCl_2$, 0.2 mM EDTA, 0.5 mM DTT, 26% glicerol (v/v), 300 mM NaCl plus serine protease inhibitors) and was incubated in ice for 30 min. Nuclear proteins were obtained by centrifugation at 20,000 g for 20 min. All samples were diluted with deionized water (1:1) and the bicinchoninic acid protein assay (BCA method) was used for protein quantification.

### 2.6. Western blot analysis

All protein extracts analyzed were from astrocyte-poor neuronal cultures. Extracts were prepared by lysing cells with RIPA buffer (150 mM NaCl, 1 mM $Na_2$EDTA, 1 mM EGTA, 20 mM Tris-HCl, pH 7.5, 1% NP-40, 1% sodium deoxycholate) plus protease inhibitors cocktail (Roche) and serine protease inhibitors (10 mM $Na_4P_2O_7$, 5 mM $Na_3VO_4$, 40 mM NaF); after 10 min incubation on ice suspensions were centrifuged for 15 min at 12,000 × *g* and protein concentration of the supernatants was determined using BCA (Thermo Scientific-Pierce). Proteins (20 μg) were resolved in 10% SDS-polyacrylamide gels by electrophoresis, transferred to nitrocellulose membranes and blocked for 1 h at 25 °C with 5% nonfat dry milk (pSerSTAT3, STAT3, β-actin) or 5% BSA (histone H1) in 0.1% Tween-20/TBS buffer (0.5 M NaCl, 20 mM Tris, pH 7.4). Membranes were incubated overnight a 4 °C with rabbit anti-pSerSTAT3 (1:1000) and mouse anti-actin (1:5000). After mild stripping, mouse anti-STAT3 (1:1000) and rabbit anti-histone H1 were added, followed by the addition of horseradish peroxidase-conjugated anti-rabbit or anti-mouse IgG antibody for 2 h at 25 °C. The immunoreactive bands were developed with peroxidase-based SuperSignal chemiluminescence assay kit (Thermo Fisher Scientific-Invitrogen) and quantified with the ImageJ software. β-actin was used as load control, and NGF was used as positive control for pSerSTAT3 activation. Band intensities were visualized by ECL (Pierce) and were densitometrically quantified using the software ImageJ.

### 2.7. Redox cytochemistry

Single-cell redox cytochemistry, to determine oxidized and reduced cysteines was performed as described [29]. In brief, astrocyte-poor neuronal cultures treated for 24 h with astrocyte-conditioned or control media were fixed for 30 min in 4% paraformaldehyde, 1 mM N-ethylmaleimide, 2 μM Alexa Fluor® 555 C5 maleimide, and 0.05% Triton X-100 prepared in PBS, pH 7.0. This pH is critical to the assay. Cells were washed three times in PBS to remove excess unreacted dye and disulfides were reduced for 30 min with 5 mM Tris(2-carboxyethyl)phosphine (TCEP) in PBS. Since TCEP reacts with maleimides, it is necessary to wash cells with PBS quickly (< 30 s). After that, cells were incubated in 1 mM N-ethylmaleimide in PBS and 2 μM Alexa Fluor® 488 C5 maleimide for 30 min. After three washing steps with PBS, the staining was completed. Cells were visualized on a Carl Zeiss LSM 710 confocal microscope using a 63 × oil objective and images were digitally acquired by using ZEN software (Zeiss). The ImageJ software was used for image analysis. All set of images were acquired with the same confocal parameters. Using the ROI manager, total neuronal areas were selected in the Alexa Fluor® 488 channel (oxidized channel) and the integrated fluorescence was measured. These areas were then transferred to the Alexa Fluor® 555 channel (reduced channel) using the overlay tool and

the same measurement was done. The total oxidation level was calculated as a ratio of intensities between the oxidized and reduced channels using the Image Calculator tool.

### 2.8. Detection of cytoplasmic hydrogen peroxide generation

Neurons from astrocyte-poor neuronal cultures ($1.5 \times 10^5$ cells/well) grown in 12 mm glass plates were transiently transfected with the HyperCyto plasmid at 7 days in vitro (DIV), using a proportion of 1:2 DNA: Lipofectamine 2000. HyperCyto is an intracellular ratiometric sensor that detects local $H_2O_2$ production [39]. Conditioned media from AβOs-stimulated astrocytes was added to the cultures after transfection and incubated for 24 h. Cells were fixed 24 h post transfection with 4% PFA/ 4% sucrose and were mounted in FluorSave reagent. Transfected neurons were excited at 488 and 405 nm and emission was collected at 505–530 nm. Fluorescence emission from excitation at 488 nm was divided by fluorescence emission at 405 nm excitation (488:405 ratio) as a measure of the $H_2O_2$ content [39]. Fluorescence emission at excitation 488 nm and excitation 405 nm varied inversely as corresponds to a ratiometric probe. Images were acquired in Carl Zeiss LSM 710 confocal microscope system using 63 × oil-immersion objective. ImageJ was used for image analysis. A mask with a specific threshold was created for the reduced (405 nm) channel, and then the reduced channel was divided by its mask. Hydrogen peroxide production was calculated as a ratio between oxidized (488 nm) and reduced (405 nm) channels using Image Calculator tool. The final image (Hyper map) was quantified. Soma and neurites were analyzed separately for each neuron.

### 2.9. Catalase, superoxide dismutase and hemoglobin treatments

In all experiments,astrocyte-rich neuronal cultures were used. The ROS-scavenger enzymes Catalase (Sigma Chem. Co. C1345) and Superoxide dismutase (Sigma Chem. Co. S5395) were diluted to 50 IU/mL, with/without AβOs, in neurobasal medium supplemented with B27; cultures were incubated for 24 h with these enzymes, which do not permeate intact polarized cells. Nitric oxide-scavenger Hemoglobin was prepared as described [40]. The reduced hemoglobin solution was immobilized in CNBr-Sepharose matrix following manufacturer's instructions. The Sepharose-hemoglobin immobilized preparation was stored in 1 M HCl for 2 weeks at 4 °C with 0.05% sodium azide. Hemoglobin concentrations were calculated as described [28].

### 2.10. Real-time qPCR

Purified primary astrocyte cultures were treated with 0.5 μM AβOs for 24 h; conditioned medium was collected after this time. Astrocyte-poor neuronal cultures were incubated with astrocyte-conditioned or control media for 24 h. Total RNA levels were determined using RNA columns; purity was assessed by the 260/280 absorbance ratio and RNA integrity by gel electrophoresis. The first cDNA strand was synthesized from total RNA (1 μg) using MLV Reverse Transcriptase. The mRNA expressions levels of STAT3 and target genes were analyzed by real-time quantitative reverse-transcription polymerase-chain-reaction (qRT-PCR). To this end, 50 ng of cDNA in 10 μL final volume was used for PCR amplification (Applied Biosystem Thermal Cycler). Amplification was performed using the appropriate primers. Sequences of primer pairs (rats) were as follow: STAT3 primers: sense 5'-CAAAG AAAACATGGCCGGCA-3' and antisense, 3'-GGGGGCTTTGTGCTTAG GAT-5' [23]; β-actin primers: sense 5'-AGGCCAACCGTGAAAAGATG-3' and antisense, 3'-ACCAGAGGCATACAGGGACAA-5' [45]; BCL2 primers: sense 5'-CTTCTCTCGTCGCTACCGTC-3' and antisense, 3'-CATG ACCCCACCGAACTCAA-5' [23]; BCL-XL primers: sense 5'-CCCAGAAG AAACTGAACCA-3' and antisense, 3'-TCACTGAATGCTCTCCGGTA-5' [59]; Survivin primers: sense 5'-TAAGCCACTTGTCCCAGCTT-3' and antisense, 3'-CTCATCCACTCCCTTCCTCA-5' [19]; BAX primers: sense 5'-TGCAGAGGATGATTGCTGA-3' and antisense, 3'-GATCAGCTCGGGC ACTTTAG-5' [59]; 18 S rRNA primers: sense 5'- GGGCCCAAGCGTTTA CTTT-3' and antisense, 3'-TTGCGCCGGTCCAAGAATTT-5'; IL-1β primers: sense 5'-TGTGATGAAAGACGGCACAC-3' and antisense, 3'- CTT CTTCTTTGGGTATTGTTTGG-5'; IL-6 primers: sense 5'-CCCTTCAGGAA CAGCTATGAA-3' and antisense, 3'- ACAACATCAGTCCCAAGAAGG-5'; TNFα primers: sense 5'-GCCCAGACCCTCACACTC-3' and antisense, 3'-CCACTCCAGCTGCTCCTCT-5'. KAPA™ SYBR® Fast qPCR reagent (KAPA Biosystems) was used in a StepOnePlus® real-time PCR equipment (Applied Biosystems, Singapore) as follows: 95 °C for 3 min, followed by 40 cycles at 95 °C for 3 s and 60 °C for 30 s, and finally a melt curve was performed at 95 °C for 15 s, for 1 min at 60 °C and 15 s at 95 °C, for detection of non-specific product formation and false-positive amplification. As an endogenous control, 18 S rRNA and β-actin expression levels were quantified. Fold-changes were quantified by using the 2(-Delta C(T)) method [38].

### 2.11. Determination of intracellular calcium signals

Astrocyte-poor neuronal cultures (~ $1.5 \times 10^5$ cells/well) grown in 25 mm glass coverslips were washed 3 times with Tyrode solution (in mM: 129 NaCl, 5 KCl, 2 $CaCl_2$, 1 $MgCl_2$, 30 Glucose, 25 HEPES-Tris, pH 7.3). Covers were loaded with 5 mM Fluo4-AM for 20 min at room temperature followed by washing, and were transferred to the microscope with 100 μL of Tyrode solution. After recording basal fluorescence for 3 min, astrocyte-conditioned or control media were added directly on top of the cover. Images of Fluo-4 fluorescence, reflecting intracellular calcium levels, were obtained in an inverted confocal microscope C2 + Spectral Nikon Eclipse TI (Plan Fluor 40 × oil DIC H N2; Fluo-4 excitation 488 nm, emission 515–520 nm), with image capture at 5 s intervals. Large fields having 60–80 cells were imaged at a given time. Frame scans were averaged using the equipment data acquisition program. Calcium signals are presented as $F/F_0$ values, where F is the experimental fluorescence and $F_0$ the basal fluorescence. Data are presented normalized with respect to the mean basal fluorescence value. Maximum fluorescence was reached after addition of the calcium ionophore ionomicyn (100 mg/mL). In all cases, the treatments did not saturate the probe. All experiments were done at room temperature.

### 2.12. BAPTA treatment

Astrocyte-poor neuronal cultures grown in 12 mm glass covers were pre-incubated with BAPTA-AM (10 μM) for 1 h before addition of astrocyte-conditioned or control media. Cells were fixed as described in the immunocytochemistry protocol.

### 2.13. Statistics

All data presented are representative of three or more independent experiments. The Shapiro-Wilk test was used for the determination of normal distribution of replicates. T-test or One-way ANOVA with Bonferroni post-hoc test were used to test for differences in mean values between different experimental conditions. A value of $p < 0.05$ was taken as statistically significant.

## 3. Results

### 3.1. The nuclear/cytoplasmic distribution of neuronal pSerSTAT3 but not of pTyrSTAT3 is affected by AβOs

Since AβOs generation causes neuronal dysfunction in AD animal models and patients, and STAT3 is an important transcription factor involved in neuronal survival in pathological conditions, we examined whether AβOs affected neuronal pSerSTAT3 nuclear distribution. Treatment of primary hippocampal cultures (7 DIV), which contain

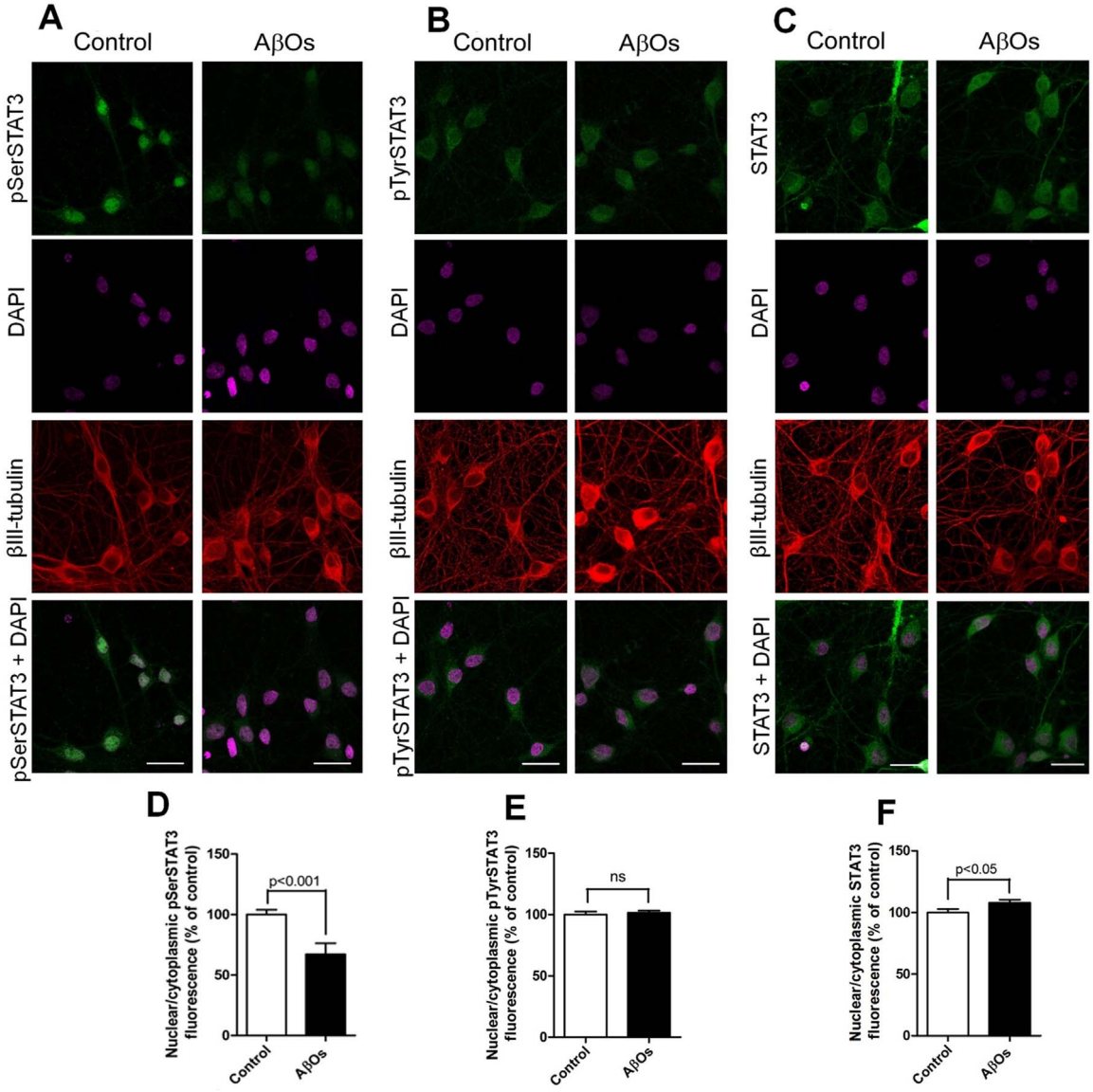


**Fig. 1.** AβOs induce a concentration dependent re-distribution of pSerSTAT3 but not of pTyrSTAT3 in astrocyte-rich neuronal cultures. Top panels: Immunostaining showing the neuronal distribution of pSerSTAT3 (**A**), pTyrSTAT3 (**B**) and STAT3 (**C**) in untreated cells and after treatment for 24 h with 0.5 μM AβOs. Scale bar: 20 μm. Quantification of nucleus/cytoplasm immunofluorescence ratio for pSerSTAT3 (**D**), pTyrSTAT3 (**E**) and STAT3 (**F**) induced by incubation for 24 h with 0.5 μM AβOs. Values represent mean ± SEM. Significance of differences was determined by two-tailed *t*-test; ns, not significant compared to the control condition.

12% of astrocytes (astrocyte-rich neuronal cultures), with the sub lethal concentration of 0.5 μM AβOs [31,44] triggered a significant re-distribution of pSerSTAT3 in neurons, identified by β-III tubulin positive staining. As illustrated in Fig. 1, treatment with 0.5 μM AβOs produced a notorious decrease of the nuclear to cytoplasmic pSerSTAT3 ratio (Fig. 1A, D). In contrast, treatment with 0.5 μM AβOs did not affect the nuclear/cytoplasmic distribution ratio of pTyrSTAT3 (Fig. 1B, E) or of total STAT3 (Fig. 1C, F). The decrease of the pSerSTAT3 nuclear/cytoplasmic ratio induced by treatment with AβOs in astrocyte-rich cultures occurred in the concentration range 0.2–0.5 μM; this inhibitory effect decreased in the 1–5 μM range (Supplementary Figure 1).

### *3.2. Astrocytes mediate the nuclear depletion of pSerSTAT3 induced by AβOs*

To determine whether reactive astrocytes play a critical role in the pSerSTAT3 redistribution elicited by AβOs, we performed parallel experiments in astrocyte-rich and astrocyte-poor neuronal cultures. To generate astrocyte-poor neuronal cultures, we incubated mixed cultures for 24 h with 1-*b*-D-arabinofuranosylcytosine (AraC). This treatment decreased the percentage of astrocytes to 4% compared to 12% in the mixed cultures (Supplementary Figure 2). We found that while AβOs (0.5 μM) significantly decreased the pSerSTAT3 nuclear to cytoplasmic ratio and decreased the overall pSerSTAT3 signal in mixed cultures, as shown by representative images (Fig. 2A) and quantification of average results (Fig. 2C), they did not affect these parameters in astrocyte-poor cultures (Fig. 2B and D). These combined results, plus the data presented in Fig. 1, suggest that the nuclear depletion of the pSerSTAT3 protein in neurons caused by AβOs requires the presence of astrocytes.

### *3.3. Treatment of astrocyte-poor neuronal cultures with AβOs did not modify pSerSTAT3 or STAT3 protein levels*

To further explore the putative role of astrocytes in pSerSTAT3 re-distribution, we examined next the effects of AβOs on STAT3 protein and mRNA levels in astrocyte-poor neuronal cultures. Treatment of these cultures with 0.5 μM AβOs for 24 h did not modify pSerSTAT3 or STAT3 protein contents (Fig. 3, A and B). In agreement with previous

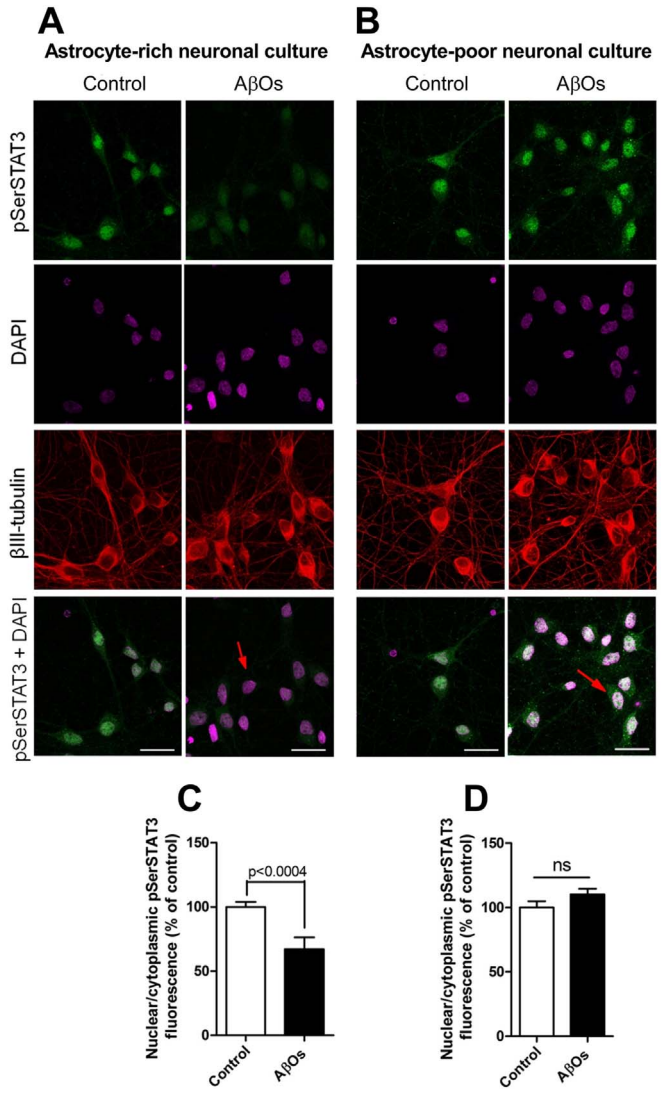


**Fig. 2.** The nuclear depletion of neuronal pSerSTAT3 induced by AβOs in mixed astrocyte-neuronal cultures depends on astrocytes. Cellular localization of neuronal pSerSTAT3 (green) after the addition of 0.5 μM AβOs for 24 h to either astrocyte-rich (**A**) or astrocyte-poor (**B**) neuronal cultures. Beta-III tubulin (red) was used as neuronal marker and DAPI (magenta) as nuclear marker. Scale bar: 20 μm. (**C**) and (**D**) Quantification of neuronal pSerSTAT3 in nucleus and cytoplasm from experiments such as those illustrated in (**A**) and (**B**), respectively. Values represent mean ± SEM from 3 independent experiments; 100 cells were analyzed for each experimental condition. Significance of differences was determined by two-tailed *t*-test. Ns, not significant compared to the control condition.

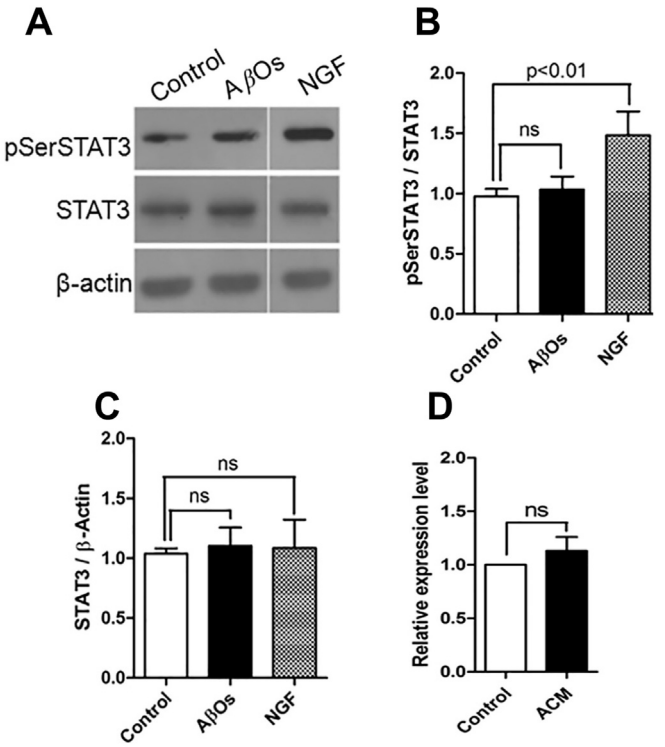


**Fig. 3.** AβOs do not affect Serine 727 phosphorylation, STAT3 protein or RNA levels in astrocyte-poor cultures. (A), pSerSTAT3, STAT3 and β-actin proteins were analyzed by western blot as described in Material and Methods. NGF was used as pSerSTAT3 inducer (positive control). (B, C), Densitometric quantification of pSerSTAT3/STAT3 ratio and STAT3/β-actin ratio after 24 h of AβOs treatment. Data are presented as fold of change compared with the basal level. Values represent mean ± SEM. Significance between differences in (A) and (B) were determined by one-way ANOVA followed by Bonferroni post-hoc test (n = 7); in (C), significance was determined by two-tailed *t*-test (n = 4).

reports [44,48], NGF produced a significant increase in pSerSTAT3 protein content, but did not affect STAT3 protein levels. We found also that treatment with AβOs did not modify STAT3 mRNA levels (Fig. 3C).

### 3.4. Treatment of astrocyte-poor neuronal cultures with astrocyte-conditioned medium (ACM) induced pSerSTAT3 nuclear depletion

To test if astrocytes release factors that promote neuronal pSerSTAT3 nuclear depletion, we prepared astrocyte-conditioned medium. To this aim, we stimulated primary astrocytes with 0.5 μM AβOs for a total period of 24 h, a treatment that in agreement with previous results [20] caused astrocyte activation, and collected the ACM to test its effects on astrocyte-poor neuronal cultures.

We found that addition of ACM to astrocyte-poor neuronal cultures did not modify STAT3 expression levels (Fig. 3D). However, measurements of pSerSTAT3 immunofluorescence in nucleus and cytoplasm after stimulation of astrocyte-rich neuronal cultures with AβOs, or of astrocyte-poor neuronal cultures with ACM revealed a significant decrease of the pSerSTAT3 immunostaining in both nucleus and cytoplasm (Fig. 4A). Similarly, western blot protein determination in isolated nucleus and cytosol revealed significantly decreased pSerSTAT3 protein levels in both fractions (Fig. 4B). Thus, although treating astrocyte-poor neuronal cultures with AβOs or ACM did not affect neuronal STAT3 mRNA or protein levels (Fig. 3), the Ser727 phosphorylation signals decreased significantly after ACM treatment (Fig. 4).

### 3.5. Mediators released by AβOs-stimulated astrocytes induced pSerSTAT3 nuclear depletion in neurons

Following Aβ stimulation *in vitro* and *in vivo,* astrocytes release ROS, pro-inflammatory cytokines and nitric oxide [2,65,69]. Thus, we tested whether ROS or nitric oxide mediate the observed effects of astrocytes on pSerSTAT3 nuclear depletion, and measured as well if AβOs-treated astrocyte released pro-inflammatory cytokines.

To test whether ROS mediate the pSerSTAT3 distribution, we co-incubated astrocyte-rich cultures with 0.5 μM A□Os plus the ROS-scavenger enzymes Superoxide dismutase (SOD) or Catalase (50 UI/mL) and tested the resulting ACM. We found that Catalase completely abolished the pSerSTAT3 nuclear depletion induced by A□Os (Fig. 5, A and B). We also found that SOD blocked the ACM effect, but further assays revealed that the SOD preparation contained peroxidase activity, so the SOD blocking effect could be ascribed to peroxidase activity contamination.

To further check whether ROS promote pSerSTAT3 nuclear depletion, we treated astrocyte-poor neuronal cultures with commercial hydrogen peroxide and found that hydrogen peroxide induced a

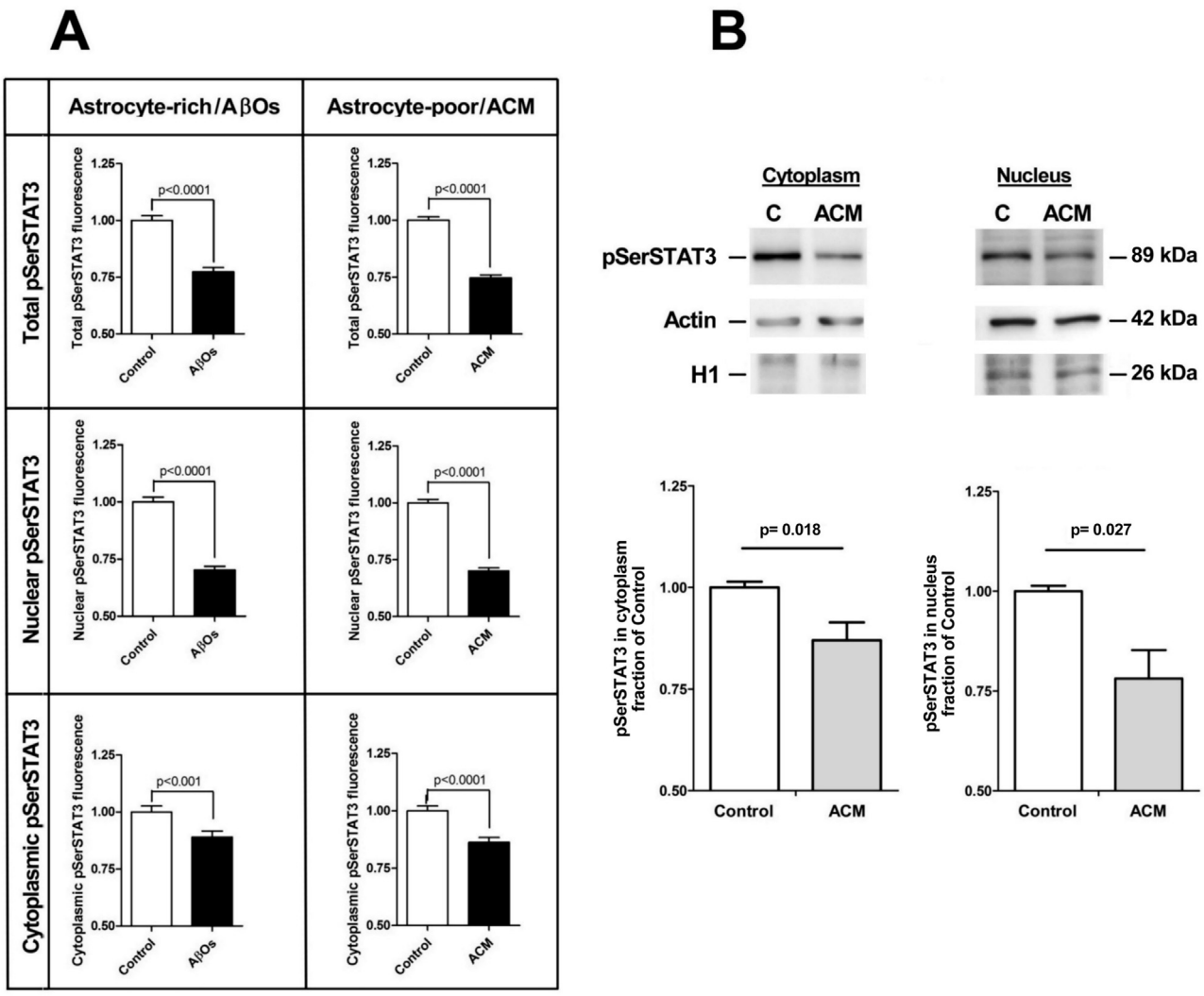


**Fig. 4.** AβOs and ACM treatment induce nuclear and cytoplasmic pSerSTAT3 dephosphorylation. (**A**) Astrocyte-rich and astrocyte-poor neuronal cultures were treated with AβOs or with ACM, respectively. Total, nuclear or cytoplasmic pSerSTAT3 immuno-labeling was quantified as described in the Methods section. A mean number of 450–500 cells was analyzed per experimental condition. Values represent mean ± SEM. Significance between differences was determined by *t*-test. (**B**) Astrocyte-poor neuronal cultures were treated with regular medium (Control) or with ACM. Cells were separated into nuclear and cytoplasmic fractions and pSerSTAT3 was determined by Western blot. As load control we used β-actin, a marker for cytoplasmic proteins, and histone H1 (H1) a marker for nuclear proteins. Graph values represent mean ± SEM from 6 independent determinations. Significance between means was evaluated by two-tailed Student *t*-test.

significant decrease of pSerSTAT3 nuclear location in neurons (Fig. 5C).

To examine whether reactive astrocytes released nitric oxide we used hemoglobin, which is a potent scavenger of nitric oxide [5]. We incubated mixed astrocyte-rich neuronal cultures with 0.5 μM AβOs in the absence or presence of 10 or 50 nM hemoglobin, and found that hemoglobin provided partial protection against the effects of AβOs (Fig. 5, D and E). We interpret this finding as an indication that nitric oxide makes a partial contribution to the oxidant agents generated by AβOs-activated astrocytes.

We further examined whether the expression of pro-inflammatory cytokines increased following treatment with AβOs of astrocyte-rich neuronal cultures, and found that 0.5 μM AβOs significantly increased IL-6 and TNF-α gene expression (Fig. 5F). Hence, AβOs treatment induced the expression of pro-inflammatory cytokines and stimulated the production of ROS and nitric oxide in astrocytes.

### *3.6. Conditioned media from AβOs-stimulated astrocytes increased neuronal oxidative tone*

Since ROS seem to be the main mediators released by AβOS-stimulated astrocytes, we evaluated if ACM treatment affected the oxidative tone in neurons. To this end, we treated astrocyte-poor neuronal cultures with ACM and measured neuronal oxidative tone using redox cytochemistry, a technique that detects changes in protein oxidation by labeling reduced cysteines with one fluorophore and reversibly oxidized cysteines with another. We found that ACM treatment produced a significant increase in the oxidation of thiol groups in neuronal proteins (Fig. 6A). Co-incubation of astrocyte-poor neuronal cultures with ACM and the antioxidant agents 3-Methyl-1-phenyl-2-pyrazolin-5-one (MCI-186), a free radical scavenger, EUK-134, a synthetic Superoxide Dismutase/Catalase mimetic, Dimethylthiourea (DMTU), a potent scavenger of hydroxyl radicals, 1-oxyl-2,2,6,6-tetramethyl-4-hydroxypiperidine (Tempol), a cytosolic permeable Superoxide Dismutase mimetic or Ethyl gallate, a hydrogen peroxide scavenger, significantly decreased in all cases the neuronal oxidation induced by ACM (Fig. 6, A and B). The antioxidants by themselves did not change neuronal oxidation levels (Fig. 6B), an indication that they counteracted specifically the effects of oxidant species present in the ACM. The pro-oxidant tert-Butyl-hydroperoxide (t-BHP) was used as positive control of oxidation (Fig. 6B).

As a second strategy to determine neuronal oxidative tone, astrocyte-poor neuronal cultures were transfected with the genetically

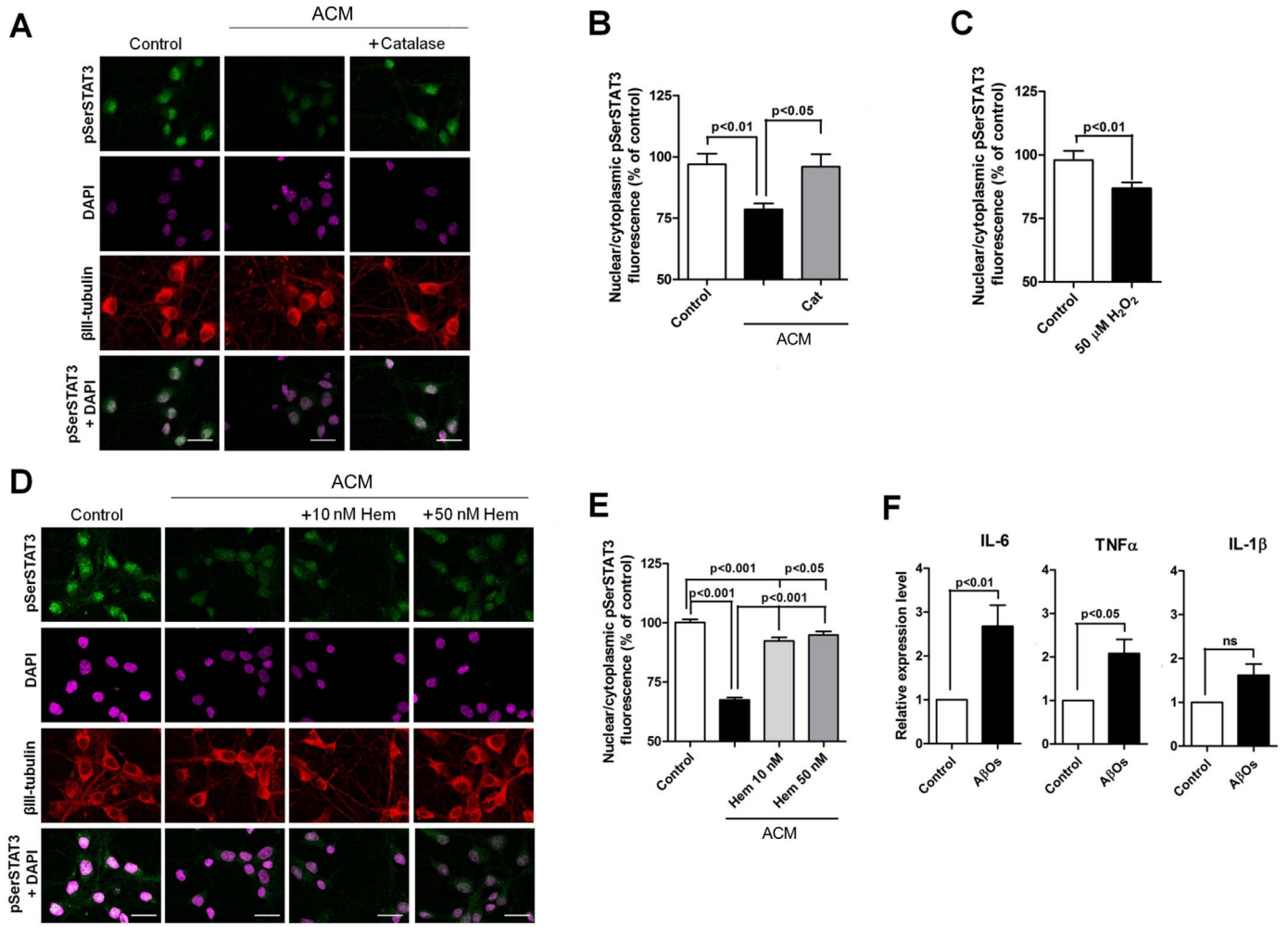


**Fig. 5.** Reactive oxygen species, nitric oxide and pro-inflammatory cytokines released by AβOs-stimulated astrocytes induce a re-distribution of pSerSTAT3 in neurons. (A), Representative images from the co-incubation of astrocyte-rich neuron cultures with AβOs and the ROS-scavenger enzyme catalase (Cat). Scale bar: 20 μm. (B), Quantification of pSerSTAT3 immunofluorescence in nucleus and cytoplasm after incubation with AβOs in the presence of Cat. Values represent mean ± SEM from three independent experiments; 100 cells were analyzed for each experimental condition. Significance between means was evaluated by one-way ANOVA. (C) Quantification of nucleus and cytoplasm immunofluorescence of pSerSTAT3 in astrocyte-poor neuronal cultures treated with 50 μM hydrogen peroxide ($H_2O_2$) for 24 h. Values represent mean ± SEM. Significance between means was evaluated using *t*-test. (D) Representative images from the co-incubation of astrocyte-rich neuronal cultures with AβOs and the nitric oxide scavenger hemoglobin. Scale bar: 20 μm. (E), Quantification of nucleus and cytoplasm immunofluorescence of pSerSTAT3 of the experiment described in (D). Values represent mean ± SEM. Significance of differences was determined by one-way ANOVA followed by Bonferroni post-hoc test. (F) mRNA levels of pro-inflammatory cytokines IL-1β, IL-6 and TNFα in AβOs-stimulated astrocytes quantified by RT-qPCR. IL-1β, IL-6 and TNFα mRNA levels were normalized by 18 S mRNA levels. Values represent mean ± SEM from seven independent experiments. Significance of differences between means was determined by *t*-test.

encoded biosensor Hyper-cyto, which detects cytoplasmic $H_2O_2$ levels [39]. We found that ACM treatment generated a significant increase in $H_2O_2$ levels in the soma and neurites of neurons (Fig. 6, C and D). To examine if treatment with antioxidant agents hinder the pSerSTAT3 redistribution induced by ACM, we co-incubated for 24 h astrocyte-poor neuronal cultures with this medium and the above antioxidant agents. We found that MCI-186, DMTU or EUK-134 abolished the re-distribution of pSerSTAT3 induced by the ACM (Fig. 6, E and F). Considering that MCI-186 and DMTU are potent hydroxyl radical scavengers and that EUK-134 is a SOD/Catalase mimetic, we suggest that hydrogen peroxide generated in neuronal cells by the ACM reacts with intracellular iron producing hydroxyl radical via the Fenton reaction, which is scavenged by MCI-186 or DMTU.

### *3.7. Conditioned media from AβOs-stimulated astrocytes generates neuronal calcium signals*

ROS and nitric oxide are important inducers of neuronal calcium signaling through the activation of intracellular and plasma membrane calcium channels [25,26,46,73]. To assess if ACM via neuronal ROS/RNS generation induces calcium signals in neurons, we measured calcium levels with Fluo4-AM in the soma of pyramidal neurons, before and after the application of ACM. Addition of this medium produced a rapid and significant intracellular calcium increase, while addition of control medium collected from astrocytes not treated with AβOs did not (Fig. 7A). To examine if calcium signals mediate the pSerSTAT3 re-distribution induced by ACM, we pre-incubated astrocyte-poor neuronal cultures with 100 μM BAPTA-AM for 1 h before incubation for 24 h with ACM or with control medium. BAPTA-AM is a cell-permeant highly selective $Ca^{2+}$ chelator that when hydrolyzed by intracellular esterases becomes membrane impermeable, thus chelating intracellular $Ca^{2+}$. We found that pre-incubation with BAPTA-AM abolished the nuclear depletion of pSerSTAT3 induced by ACM (Fig. 7B), and that pre-incubation with BAPTA-AM by itself did not modify pSerSTAT3 nuclear/cytoplasmic distribution (Fig. 7B). Based on these results, we propose that the increase in intracellular calcium levels is essential for the pSerSTAT3 redistribution induced by the ACM.

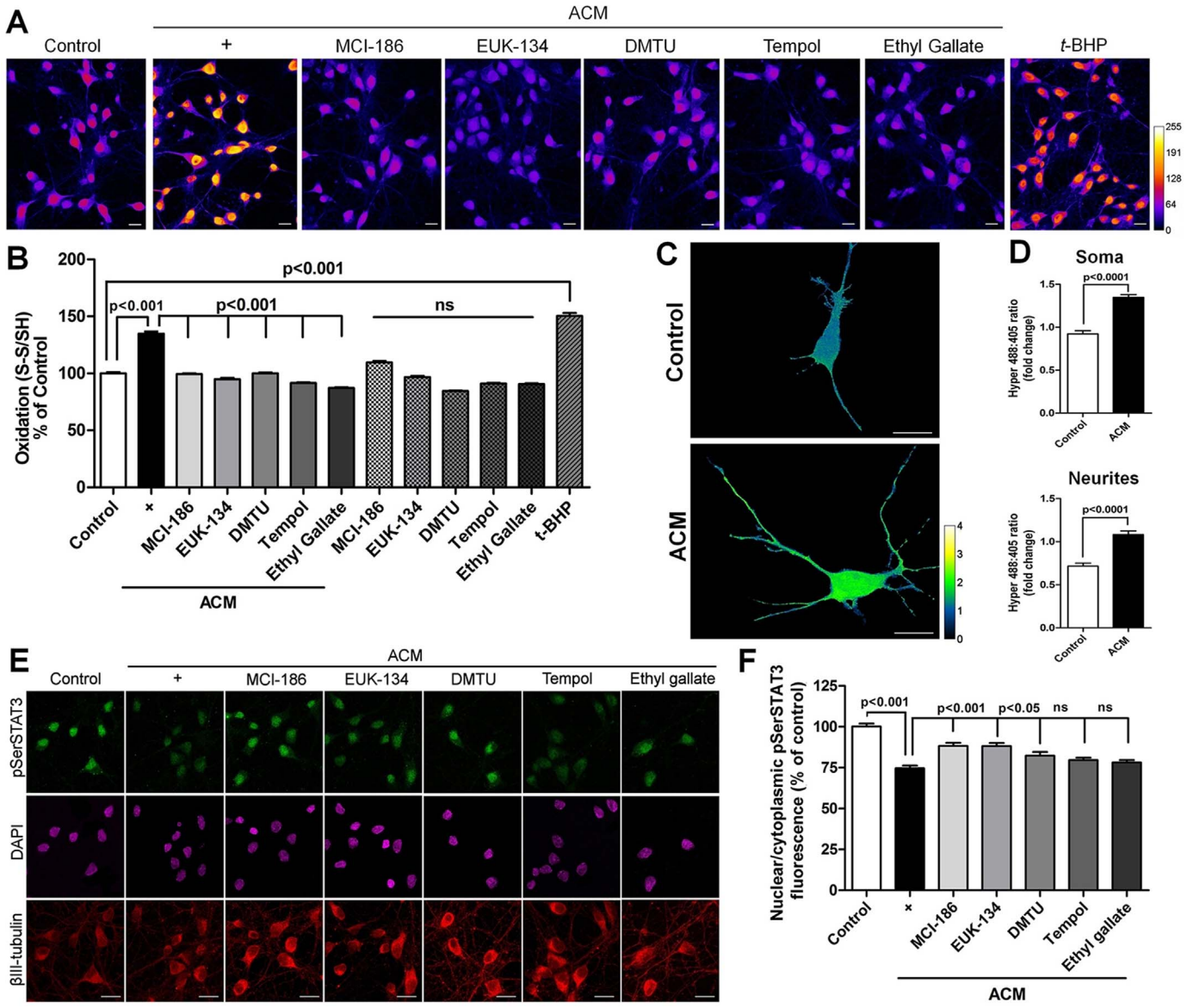


**Fig. 6.** Treatment with ACM increases the oxidative tone in neurons and antioxidant agents abolish this effect. (A), Representative images collected in the channel that determines oxidized (S-S) cysteines (see Methods) after addition of ACM or control media, in the absence or presence of the antioxidants MCI186, EUK134, dimethylthiourea (DMTU), Tempol or ethyl gallate. The pro-oxidant agent tert-Butyl hydroperoxide (t-BHP) was used as positive control. S-S fluorescence intensity was transformed into a thermal scale (ImageJ program) in which a shift from blue to white indicates increasing degrees of oxidation (lower right-hand bar). (B), Quantification of the oxidized/reduced (S-S/S-H) ratio was performed as described in Methods. Values represent mean ± SEM. Significance of differences between means were determined by one-way ANOVA, followed by Bonferroni post-hoc test; three independent experiments. (C), Representative images of Hyper-cyto fluorescence determined in astrocyte-poor neuronal cultures treated with ACM. Hyper-cyto fluorescence intensity was transformed into a thermal scale (lower right-hand bar in lower panel) in which a shift from blue to green to yellow indicates increasing degrees of oxidation. Scale bar: 10 μm. (D) The graph represents quantification of fluorescence levels in soma and neurites. Values represent mean ± SEM. Significance of differences between means was determined by *t*-test in three independent experiments. (E), Representative images of pSerSTAT3 nuclear/cytoplasm distribution in astrocyte-poor neuronal cultures treated with ACM and the antioxidants MCI186, EUK134, dimethylthiourea (DMTU), Tempol or ethyl gallate. MCI186, EUK134 and DMTU abolished the ACM-induced pSerSTAT3 nuclear depletion. Scale bar: 10 μm. (F), Quantification of the experiment shown in (E). Values represent mean ± SEM. Significance of differences between means were determined by one-way ANOVA, followed by Bonferroni post-hoc test; three independent experiments.

### *3.8. Conditioned media from AβOs-stimulated astrocytes decreases STAT3-target survival genes and increases the pro-apoptotic BAX/BCL2 ratio in neurons*

STAT3 is a transcription factor whose activity is modified by oxidative stress. Previous studies have postulated that under different oxidative stimuli STAT3 undergoes thiol oxidation in critical cysteines involved in DNA interaction [9,36], suggesting that oxidation of STAT3 affects its transcriptional activity. To assess if ACM modifies STAT3 transcriptional activity, we measured the expression levels of different STAT3-target survival genes by real-time PCR. We found that the expression of BCL2 and Survivin were significantly decreased in response to treatment with ACM, whereas the expression of BCL-XL, another member of the BCL2-family, showed a tendency to decrease (Fig. 8A). Furthermore, this conditioned medium produced an increase in the BAX/BCL2 ratio, which is a classical pro-apoptotic signal (Fig. 8B). Based on the effect of extracellular ROS scavengers (catalase, hemoglobin) and the effect of cell-permeant antioxidants and BAPTA, we propose that oxidants released by AβOs-stimulated astrocytes impair STAT3 neuroprotective activity through a calcium-mediated process.

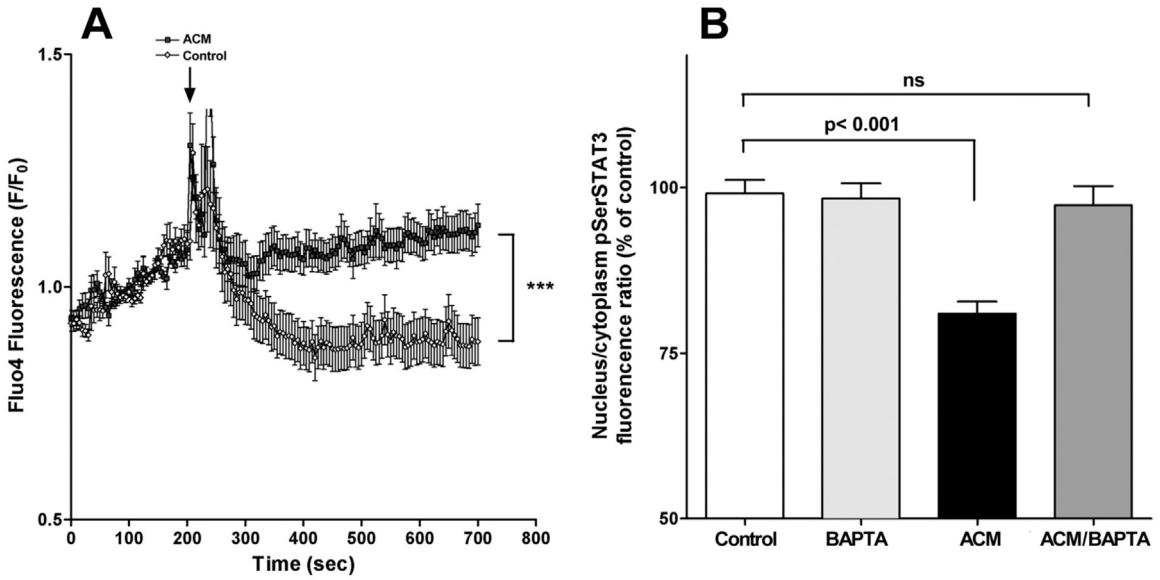


**Fig. 7.** The ACM induces calcium signals; intracellular calcium chelation abolishes pSerSTAT3 relocation. (**A**), Astrocyte-poor neuronal cultures were loaded with the calcium sensor Fluo-4 and then challenged with ACM or control medium. Calcium signals were recorded as a function of time in an inverted confocal microscope, and were quantified using the equipment data acquisition program. Values represent mean ± SEM of Fluo-4 fluorescence determined in 45 individual cells per experimental condition. Significance of differences between means was determined by *t*-test; ***: $p < 0.001$. (**B**), Astrocyte-poor neuronal cultures were pre-incubated with or without 100 μM BAPTA-AM for 1 h before incubation for 24 h with astrocyte-conditioned or control media. Cells were immunostained for pSerSTAT3 and the nucleus/cytoplasm fluorescence ratio was determined as described in Methods. Values represent mean ± SEM from three independent experiments; on average 100 cells were analyzed for each experimental condition. Significance between differences was determined by one-way ANOVA followed by Bonferroni post-hoc test.

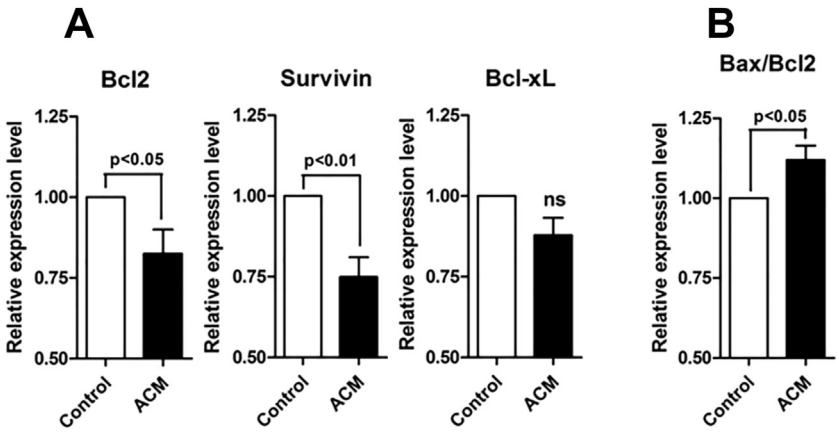


**Fig. 8.** ACM decreases STAT3 survival-target genes and increases the pro-apoptotic BAX/BCL2 ratio in neurons. **(A)** BCL2, Survivin, BCL-XL and BAX mRNA were quantified by qRT-PCR in astrocyte-poor neuronal cultures treated with ACM. All mRNA values were normalized by β-actin mRNA levels. Values represent mean ± SEM. Significance of differences was determined by *t*-test. Results are from seven independent experiments. (**B**) Pro-apoptotic BAX/BCL2 ratio. Values represent mean ± SEM from seven independent experiments. Significance of differences was determined by *t*-test.

## 4. Discussion

We explored in this study the interplay between AβOs, astrocytes and neurons, and tested if AβOs-stimulated astrocytes affect neuronal viability genes. The results highlight the pSerSTAT3 form of STAT3 as critical for the expression of neuronal genes, whose activity is hindered by AβOs-stimulated astrocytes.

Full transcriptional activity of STAT3 depends on the presence of pSerSTAT3. Nevertheless, the factors that determine pSerSTAT3 nuclear location are largely unknown. We found that treatment of astrocyte-rich neuronal cultures with sub-lethal concentrations of AβOs decreased the nuclear distribution of pSerSTAT3. An inverse relationship was observed in the 0.05–0.2 μM range of AβOs concentration. In contrast, higher AβOs concentrations did not modify pSerSTAT3 nuclear distribution when compared to control. We hypothesize that the observed lack of effect of higher AβOs concentrations is probably due to the formation of less active polymorphic fibril aggregates, a process that is highly favored by increasing Aβ concentration [61].

### *4.1. Astrocyte-neuron interaction mediates AβOs-induced pSerSTAT3 nuclear depletion*

Treatment of astrocyte-rich neuronal cultures with AβOs did not change total STAT3 or pTyrSTAT3 nuclear distribution, pointing to a specific effect of AβOs on the nuclear depletion of the pSerSTAT3 form. Hence, we conclude that this depletion requires the presence of astrocytes since it did not occur in astrocyte-poor neuronal cultures. In support of this conclusion, we observed that ACM addition to astrocyte-poor neuronal cultures caused similar pSerSTAT3 nuclear depletion as that observed in astrocyte-rich neuronal cultures. Moreover, these findings indicate that AβOs-treated astrocytes release agents that mediate pSerSTAT3 nuclear depletion. These findings are in agreement with pioneering work showing that the Aβ peptide acts preferentially on astrocytes but causes neuronal death [2], and highlight the role of astrocytes in AβOs-induced neuronal degeneration.

Importantly, total neuronal pSerSTAT3 levels decreased markedly after treatment of astrocyte-rich neuronal cultures with AβOs or after treatment of astrocyte-poor neuronal cultures with ACM. Based on these results, we strongly suggest that the neuronal ROS increase

produced by AβOs-treated astrocytes induce calcium signals that recruit calcium-dependent serine phosphatases such as calcineurin [51], which catalyze pSerSTAT3 dephosphorylation. Arguably, pSerSTAT3 dephosphorylation could result from the sequence AβOs activation of astrocytes – ROS release – neuronal ROS and calcium upsurge – calcineurin activation. Alternatively, the ROS-calcium signal axis may inhibit the activity of phosphoserine kinases germane to pSerSTAT3 phosphorylation. The ROS-induced neuronal calcium upsurge could be mediated either by the highly redox-sensitive ryanodine receptor calcium channels [16] or by transient receptor potential canonical 6 calcium channels [32,56].

### 4.2. Reactive oxygen species mediate the effects of AβOs-stimulated astrocytes

Previous work has shown that AβOs induce calcium signaling in astrocytes, and that AβOs treatment decreased the level of reduced glutathione in both neurons and astrocytes [4]. We found that AβOs treatment of astrocytes induced a reactive phenotype that released ROS and RNS and displayed increased IL-6 and TNFα transcriptional activity. These observations are in agreement with literature reports describing pro-inflammatory phenotype emergence in AβOs-stimulated astrocytes [11,69]. Similarly, previous reports have shown that AβOs induce calcium signals in astrocytes, which result in NOX activation and increased ROS production and nitric oxide release. In this work, we found that treatment of astrocyte-poor neuronal cultures with ACM significantly increased $H_2O_2$ levels in neuronal soma and neurites, and promoted a significant increase in oxidized neuronal protein content. In addition, we observed that SOD, a superoxide scavenger enzyme, or catalase, a hydrogen peroxide scavenger enzyme, abolished the pSerSTAT3 nuclear depletion produced by ACM, indicating that ROS released by AβOs-treated astrocytes mediate this depletion. Since AβOs induce NOX activity [2,70], it is likely that astrocytic NOX, activated by AβOs, acts as the source of hydrogen peroxide in ACM.

Scavenging of nitric oxide decreased the effects of ACM, although not as effectively as ROS scavenging. The most probable mechanism accounting for the putative secretion of nitric oxide by AβOs-stimulated astrocytes would be iNOS activation by a process that also requires the participation of inflammatory cytokines [3,50,63]. In agreement with previous literature reports, we found that AβOs treatment significantly increased the expression of the pro-inflammatory cytokines IL-6 and TNF-α in astrocytes. Hence, a circuit engaging cytokine production and iNOS activation may mediate, at least in part, nitric oxide production by AβOs-stimulated astrocytes.

### 4.3. Neuronal calcium signals mediate the nuclear depletion of pSerSTAT3 induced by ACM

ROS and nitric oxide are important inducers of neuronal calcium signaling through the activation of intracellular and plasma membrane calcium channels [46,73]. Considering that ROS increase intracellular calcium levels in neurons, we tested the possible involvement of calcium signals on pSerSTAT3 nuclear relocation. We found that astrocyte-conditioned medium induced calcium signals and that intracellular calcium chelation with BAPTA prevented pSerSTAT3 nuclear depletion. As expected, pre-treatment of the cells with antioxidants completely abolished the calcium response to ACM (Supplementary Figure 3). We propose, based on these overall results, that ROS-induced calcium signals mediate the neuronal pSerSTAT3 depletion induced by ACM.

### 4.4. Decreased pSerSTAT3 nuclear distribution results in decreased expression of STAT3 survival target genes

We found that the expression of BCL2 and Survivin were significant decreased in response to treatment of astrocyte-poor neuronal cultures with ACM. Furthermore, treatment with ACM increased the BAX/BCL2 ratio, while BCL-XL showed a tendency to decrease. We suggest, accordingly, that nuclear pSerSTAT3 promotes the expression of anti-apoptotic genes, and that pro-oxidant species released by AβOs-treated astrocytes trigger signaling cascades that diminish this activity by depleting pSerSTAT3 from the nucleus.

In summary, we propose that AβOs-activated astrocytes release oxidative mediators that specifically decrease the nuclear/cytoplasmic distribution of pSerSTAT3 in neurons through sequential increases in intracellular ROS and calcium, with the consequent decrease in the expression of survival STAT3-target genes.

## Acknowledgments

This work was supported by FONDECYT Chile grant 1150736, BNI grant P-09-015F, Program for Research, Faculty of Sciences of the Universidad de Chile (PAIFAC), and U-APOYA 2236, VID, Universidad de Chile. YM was supported by Doctoral fellowship 21130445 from CONICYT, Chile. We thank Dr. Cecilia Hidalgo for critical reading of the article.

## Author disclosure statement

No competing financial interests exist.

## Appendix A. Supporting information

Supplementary data associated with this article can be found in the online version at http://dx.doi.org/10.1016/j.freeradbiomed.2018.01.006.

## References

[1] A.Y. Abramov, L. Canevari, M.R. Duchen, Beta-amyloid peptides induce mitochondrial dysfunction and oxidative stress in astrocytes and death of neurons through activation of NADPH oxidase, J. Neurosci. 24 (2004) 565–575.
[2] A.Y. Abramov, M.R. Duchen, The role of an astrocytic NADPH oxidase in the neurotoxicity of amyloid beta peptides, Philos. Trans. R. Soc. Lond. B Biol. Sci. 360 (2005) 2309–2314.
[3] K.T. Akama, C. Albanese, R.G. Pestell, L.J. Van Eldik, Amyloid beta-peptide stimulates nitric oxide production in astrocytes through an NFkappaB-dependent mechanism, Proc. Natl. Acad. Sci. USA 95 (1998) 5795–5800.
[4] P.R. Angelova, A.Y. Abramov, Interaction of neurons and astrocytes underlies the mechanism of Abeta-induced neurotoxicity, Biochem. Soc. Trans. 42 (2014) 1286–1290.
[5] I. Azarov, K.T. Huang, S. Basu, M.T. Gladwin, N. Hogg, D.B. Kim-Shapiro, Nitric oxide scavenging by red blood cells as a function of hematocrit and oxygenation, J. Biol. Chem. 280 (2005) 39024–39032.
[6] L. Ben Haim, K. Ceyzeriat, M.A. Carrillo-de Sauvage, F. Aubry, G. Auregan, M. Guillermier, M. Ruiz, F. Petit, D. Houitte, E. Faivre, M. Vandesquille, R. Aron-Badin, M. Dhenain, N. Deglon, P. Hantraye, E. Brouillet, G. Bonvento, C. Escartin, The JAK/STAT3 pathway is a common inducer of astrocyte reactivity in Alzheimer's and Huntington's diseases, J. Neurosci. 35 (2015) 2817–2829.
[7] C. Benito, C.M. Davis, J.A. Gomez-Sanchez, M. Turmaine, D. Meijer, V. Poli, R. Mirsky, K.R. Jessen, STAT3 controls the long-term survival and phenotype of repair schwann cells during nerve regeneration, J. Neurosci. 37 (2017) 4255–4269.
[8] E. Butturini, A. Carcereri de Prati, G. Chiavegato, A. Rigo, E. Cavalieri, E. Darra, S. Mariotto, Mild oxidative stress induces S-glutathionylation of STAT3 and enhances chemosensitivity of tumoural cells to chemotherapeutic drugs, Free Radic. Biol. Med. 65 (2013) 1322–1330.
[9] E. Butturini, E. Darra, G. Chiavegato, B. Cellini, F. Cozzolino, M. Monti, P. Pucci, D. Dell'Orco, S. Mariotto, S-Glutathionylation at Cys328 and Cys542 impairs STAT3 phosphorylation, ACS Chem. Biol. 9 (2014) 1885–1893.
[10] M. Carballo, M. Conde, R. El Bekay, J. Martin-Nieto, M.J. Camacho, J. Monteseirin, J. Conde, F.J. Bedoya, F. Sobrino, Oxidative stress triggers STAT3 tyrosine phosphorylation and nuclear translocation in human lymphocytes, J. Biol. Chem. 274 (1999) 17580–17586.
[11] I. Carrero, M.R. Gonzalo, B. Martin, J.M. Sanz-Anquela, J. Arevalo-Serrano, A. Gonzalo-Ruiz, Oligomers of beta-amyloid protein (Abeta1-42) induce the activation of cyclooxygenase-2 in astrocytes via an interaction with interleukin-1beta, tumour necrosis factor-alpha, and a nuclear factor kappa-B mechanism in the rat brain, Exp. Neurol. 236 (2012) 215–227.
[12] T. Chiba, M. Yamada, J. Sasabe, K. Terashita, M. Shimoda, M. Matsuoka, S. Aiso, Amyloid-beta causes memory impairment by disturbing the JAK2/STAT3 axis in hippocampal neurons, Mol. Psychiatry 14 (2009) 206–222.
[13] J.E. Darnell Jr., STATs and gene regulation, Science 277 (1997) 1630-5.
[14] T. Decker, P. Kovarik, Serine phosphorylation of STATs, Oncogene 19 (2000)

2628–2637.
[15] B.E. Deverman, P.H. Patterson, Cytokines and CNS development, Neuron 64 (2009) 61–78.
[16] P. Donoso, G. Sanchez, R. Bull, C. Hidalgo, Modulation of cardiac ryanodine receptor activity by ROS and RNS, Front. Biosci. (Landmark Ed.) 16 (2011) 553–567.
[17] S. Dziennis, N.J. Alkayed, Role of signal transducer and activator of transcription 3 in neuronal survival and regeneration, Rev. Neurosci. 19 (2008) 341–361.
[18] M. Eufemi, R. Cocchiola, D. Romaniello, V. Correani, L. Di Francesco, C. Fabrizi, B. Maras, M.E. Schinina, Acetylation and phosphorylation of STAT3 are involved in the responsiveness of microglia to beta amyloid, Neurochem. Int. 81 (2015) 48–56.
[19] Z. Fan, B. Liu, S. Zhang, H. Liu, Y. Li, D. Wang, Y. Liu, J. Li, N. Wang, Y. Liu, B. Zhang, YM155, a selective survivin inhibitor, reverses chronic hypoxic pulmonary hypertension in rats via upregulating voltage-gated potassium channels, Clin. Exp. Hypertens. 37 (2015) 381–387.
[20] L. Forny-Germano, N.M. Lyra e Silva, A.F. Batista, J. Brito-Moreira, M. Gralle, S.E. Boehnke, B.C. Coe, A. Lablans, S.A. Marques, A.M. Martinez, W.L. Klein, J.C. Houzel, S.T. Ferreira, D.P. Munoz, F.G. De Felice, Alzheimer's disease-like pathology induced by amyloid-beta oligomers in nonhuman primates, J. Neurosci. 34 (2014) 13629–13643.
[21] A.J. Garcia-Yague, P. Rada, A.I. Rojo, I. Lastres-Becker, A. Cuadrado, Nuclear import and export signals control the subcellular localization of Nurr1 protein in response to oxidative stress, J. Biol. Chem. 288 (2013) 5506–5517.
[22] C.K. Glass, K. Saijo, B. Winner, M.C. Marchetto, F.H. Gage, Mechanisms underlying inflammation in neurodegeneration, Cell 140 (2010) 918–934.
[23] M.M. Hafez, N.O. Al-Harbi, A.R. Al-Hoshani, K.A. Al-Hosaini, S.D. Al Shrari, S.S. Al Rejaie, M.M. Sayed-Ahmed, O.A. Al-Shabanah, Hepato-protective effect of rutin via IL-6/STAT3 pathway in CCl4-induced hepatotoxicity in rats, Biol. Res. 48 (2015) 30.
[24] G. He, M.N.F.-kappaB. Karin, and STAT3 - key players in liver inflammation and cancer, Cell Res. 21 (2011) 159–168.
[25] C. Hidalgo, M.A. Carrasco, P. Munoz, M.T. Nunez, A role for reactive oxygen/nitrogen species and iron on neuronal synaptic plasticity, Antioxid. Redox Signal. 9 (2007) 245–255.
[26] C. Hidalgo, P. Donoso, Crosstalk between calcium and redox signaling: from molecular mechanisms to health implications, Antioxid. Redox Signal. 10 (2008) 1275–1312.
[27] E.J. Hillmer, H. Zhang, H.S. Li, S.S. Watowich, STAT3 signaling in immunity, Cytokine Growth Factor Rev. 31 (2016) 1–15.
[28] S. Hindley, B.H. Juurlink, J.W. Gysbers, P.J. Middlemiss, M.A. Herman, M.P. Rathbone, Nitric oxide donors enhance neurotrophin-induced neurite outgrowth through a cGMP-dependent mechanism, J. Neurosci. Res. 47 (1997) 427–439.
[29] M.P. Horowitz, C. Milanese, R. Di Maio, X. Hu, L.M. Montero, L.H. Sanders, V. Tapias, S. Sepe, W.A. van Cappellen, E.A. Burton, J.T. Greenamyre, P.G. Mastroberardino, Single-cell redox imaging demonstrates a distinctive response of dopaminergic neurons to oxidative insults, Antioxid. Redox Signal. 15 (2011) 855–871.
[30] J.E. Jung, G.S. Kim, P. Narasimhan, Y.S. Song, P.H. Chan, Regulation of Mn-superoxide dismutase activity and neuroprotection by STAT3 in mice after cerebral ischemia, J. Neurosci. 29 (2009) 7003–7014.
[31] S. Kaech, G. Banker, Culturing hippocampal neurons, Nat. Protoc. 1 (2006) 2406–2415.
[32] E.Y. Kim, M. Anderson, S.E. Dryer, Sustained activation of N-methyl-D-aspartate receptors in podocytes leads to oxidative stress, mobilization of transient receptor potential canonical 6 channels, nuclear factor of activated T cells activation, and apoptotic cell death, Mol. Pharmacol. 82 (2012) 728–737.
[33] M.Y. Koo, J. Park, J.M. Lim, S.Y. Joo, S.P. Shin, H.B. Shim, J. Chung, D. Kang, H.A. Woo, S.G. Rhee, Selective inhibition of the function of tyrosine-phosphorylated STAT3 with a phosphorylation site-specific intrabody, Proc. Natl. Acad. Sci. USA 111 (2014) 6269–6274.
[34] P.N. Lacor, M.C. Buniel, P.W. Furlow, A.S. Clemente, P.T. Velasco, M. Wood, K.L. Viola, W.L. Klein, Abeta oligomer-induced aberrations in synapse composition, shape, and density provide a molecular basis for loss of connectivity in Alzheimer's disease, J. Neurosci. 27 (2007) 796–807.
[35] M.P. Lambert, A.K. Barlow, B.A. Chromy, C. Edwards, R. Freed, M. Liosatos, T.E. Morgan, I. Rozovsky, B. Trommer, K.L. Viola, P. Wals, C. Zhang, C.E. Finch, G.A. Krafft, W.L. Diffusible Klein, nonfibrillar ligands derived from Abeta1-42 are potent central nervous system neurotoxins, Proc. Natl. Acad. Sci. USA 95 (1998) 6448–6453.
[36] L. Li, S.H. Cheung, E.L. Evans, P.E. Shaw, Modulation of gene expression and tumor cell growth by redox modification of STAT3, Cancer Res. 70 (2010) 8222–8232.
[37] L. Li, P.E. Shaw, A STAT3 dimer formed by inter-chain disulphide bridging during oxidative stress, Biochem. Biophys. Res. Commun. 322 (2004) 1005–1011.
[38] K.J. Livak, T.D. Schmittgen, Analysis of relative gene expression data using real-time quantitative PCR and the 2(-Delta Delta C(T)) Method, Methods 25 (2001) 402–408.
[39] K.A. Lukyanov, V.V. Belousov, Genetically encoded fluorescent redox sensors, Biochim. Biophys. Acta 745–56 (1840) 2014.
[40] W. Martin, G.M. Villani, D. Jothianandan, R.F. Furchgott, Selective blockade of endothelium-dependent and glyceryl trinitrate-induced relaxation by hemoglobin and by methylene blue in the rabbit aorta, J. Pharmacol. Exp. Ther. 232 (1985) 708–716.
[41] C. Maziere, G. Alimardani, F. Dantin, F. Dubois, M.A. Conte, J.C. Maziere, Oxidized LDL activates STAT1 and STAT3 transcription factors: possible involvement of reactive oxygen species, FEBS Lett. 448 (1999) 49–52.
[42] S. Murase, E. Kim, L. Lin, D.A. Hoffman, R.D. McKay, Loss of signal transducer and activator of transcription 3 (STAT3) signaling during elevated activity causes vulnerability in hippocampal neurons, J. Neurosci. 32 (2012) 15511–15520.
[43] P. Narayan, K.M. Holmstrom, D.H. Kim, D.J. Whitcomb, M.R. Wilson, P. St George-Hyslop, N.W. Wood, C.M. Dobson, K. Cho, A.Y. Abramov, D. Klenerman, Rare individual amyloid-beta oligomers act on astrocytes to initiate neuronal damage, Biochemistry 53 (2014) 2442–2453.
[44] Y.P. Ng, Z.H. Cheung, N.Y. Ip, STAT3 as a downstream mediator of Trk signaling and functions, J. Biol. Chem. 281 (2006) 15636–15644.
[45] L. Pang, Y. Cai, E.H. Tang, D. Yan, R. Kosuru, H. Li, M.G. Irwin, H. Ma, Z. Xia, Cox-2 inhibition protects against Hypoxia/Reoxygenation-induced cardiomyocyte apoptosis via Akt-dependent enhancement of iNOS expression, Oxid. Med. Cell. Longev. (2016) 3453059 (2016).
[46] A.C. Paula-Lima, T. Adasme, C. Hidalgo, Contribution of Ca2+ release channels to hippocampal synaptic plasticity and spatial memory: potential redox modulation, Antioxid. Redox Signal. 21 (2014) 892–914.
[47] A.C. Paula-Lima, T. Adasme, C. SanMartin, A. Sebollela, C. Hetz, M.A. Carrasco, S.T. Ferreira, C. Hidalgo, Amyloid beta-peptide oligomers stimulate RyR-mediated Ca2+ release inducing mitochondrial fragmentation in hippocampal neurons and prevent RyR-mediated dendritic spine remodeling produced by BDNF, Antioxid. Redox Signal. 14 (2011) 1209–1223.
[48] M.J. Pellegrino, B.A. Habecker, STAT3 integrates cytokine and neurotrophin signals to promote sympathetic axon regeneration, Mol. Cell. Neurosci. 56 (2013) 272–282.
[49] Y. Qu, A.M. Oyan, R. Liu, Y. Hua, J. Zhang, R. Hovland, M. Popa, X. Liu, K.A. Brokstad, R. Simon, A. Molven, B. Lin, W.D. Zhang, E. McCormack, K.H. Kalland, X.S. Ke, Generation of prostate tumor-initiating cells is associated with elevation of reactive oxygen species and IL-6/STAT3 signaling, Cancer Res 73 (2013) 7090–7100.
[50] F. Rossi, E. Bianchini, Synergistic induction of nitric oxide by beta-amyloid and cytokines in astrocytes, Biochem. Biophys. Res. Commun. 225 (1996) 474–478.
[51] S. Saito, Y. Hiroi, Y. Zou, R. Aikawa, H. Toko, F. Shibasaki, Y. Yazaki, R. Nagai, I. Komuro, beta-Adrenergic pathway induces apoptosis through calcineurin activation in cardiac myocytes, J. Biol. Chem. 275 (2000) 34528–34533.
[52] R. Sattler, J.D. Rothstein, Regulation and dysregulation of glutamate transporters, Handb. Exp. Pharmacol. (2006) 277–303.
[53] U. Schweizer, J. Gunnersen, C. Karch, S. Wiese, B. Holtmann, K. Takeda, S. Akira, M. Sendtner, Conditional gene ablation of Stat3 reveals differential signaling requirements for survival of motoneurons during development and after nerve injury in the adult, J. Cell Biol. 156 (2002) 287–297.
[54] G. Seifert, K. Schilling, C. Steinhauser, Astrocyte dysfunction in neurological disorders: a molecular perspective, Nat. Rev. Neurosci. 7 (2006) 194–206.
[55] Y. Shen, K. Schlessinger, X. Zhu, E. Meffre, F. Quimby, D.E. Levy, J.E. Darnell Jr., Essential role of STAT3 in postnatal survival and growth revealed by mice lacking STAT3 serine 727 phosphorylation, Mol. Cell. Biol. 24 (2004) 407–419.
[56] S. Shimizu, N. Takahashi, Y. Mori, TRPs as chemosensors (ROS, RNS, RCS, gasotransmitters), Handb. Exp. Pharmacol. 223 (2014) 767–794.
[57] M. Simard, M. Nedergaard, The neurobiology of glia in the context of water and ion homeostasis, Neuroscience 129 (2004) 877–896.
[58] A.R. Simon, U. Rai, B.L. Fanburg, B.H. Cochran, Activation of the JAK-STAT pathway by reactive oxygen species, Am. J. Physiol. 275 (1998) C1640–C1652.
[59] G. Singh-Mallah, C.D. McMahon, J. Guan, K. Singh, Cyclic-glycine-proline accelerates mammary involution by promoting apoptosis and inhibiting IGF-1 function, J. Cell. Physiol. (2017).
[60] M.C. Sobotta, W. Liou, S. Stocker, D. Talwar, M. Oehler, T. Ruppert, A.N. Scharf, T.P. Dick, Peroxiredoxin-2 and STAT3 form a redox relay for H2O2 signaling, Nat. Chem. Biol. 11 (2015) 64–70.
[61] W.B. Stine Jr., K.N. Dahlgren, G.A. Krafft, M.J. LaDu, In vitro characterization of conditions for amyloid-beta peptide oligomerization and fibrillogenesis, J. Biol. Chem. 278 (2003) 11612–11622.
[62] K. Takeda, K. Noguchi, W. Shi, T. Tanaka, M. Matsumoto, N. Yoshida, T. Kishimoto, S. Akira, Targeted disruption of the mouse Stat3 gene leads to early embryonic lethality, Proc. Natl. Acad. Sci. USA 94 (1997) 3801–3804.
[63] P.J. Urrutia, E.C. Hirsch, C. Gonzalez-Billault, M.T. Nunez, Hepcidin attenuates amyloid beta-induced inflammatory and pro-oxidant responses in astrocytes and microglia, J. Neurochem. (2017).
[64] B. Viviani, Preparation and coculture of neurons and glial cells (Unit2.7), Curr. Protoc. Cell Biol. (2006) (Unit2.7).
[65] M.N. Wallace, J.G. Geddes, D.A. Farquhar, M.R. Masson, Nitric oxide synthase in reactive astrocytes adjacent to beta-amyloid plaques, Exp. Neurol. 144 (1997) 266–272.
[66] J. Wan, A.K. Fu, F.C. Ip, H.K. Ng, J. Hugon, G. Page, J.H. Wang, K.O. Lai, Z. Wu, N.Y. Ip, Tyk2/STAT3 signaling mediates beta-amyloid-induced neuronal cell death: implications in Alzheimer's disease, J. Neurosci. 30 (2010) 6873–6881.
[67] Z. Wen, J.E. Darnell Jr., Mapping of Stat3 serine phosphorylation to a single residue (727) and evidence that serine phosphorylation has no influence on DNA binding of Stat1 and Stat3, Nucleic Acids Res. 25 (1997) 2062–2067.
[68] Z. Wen, Z. Zhong, J.E. Darnell Jr., Maximal activation of transcription by Stat1 and Stat3 requires both tyrosine and serine phosphorylation, Cell 82 (1995) 241–250.
[69] J.A. White, A.M. Manelli, K.H. Holmberg, L.J. Van Eldik, M.J. Ladu, Differential effects of oligomeric and fibrillar amyloid-beta 1-42 on astrocyte-mediated inflammation, Neurobiol. Dis. 18 (2005) 459–465.
[70] A. Wyssenbach, T. Quintela, F. Llavero, J.L. Zugaza, C. Matute, E. Alberdi, Amyloid beta-induced astrogliosis is mediated by beta1-integrin via NADPH oxidase 2 in Alzheimer's disease, Aging Cell (2016).
[71] Y. Xie, S. Kole, P. Precht, M.J. Pazin, M. Bernier, S-glutathionylation impairs signal transducer and activator of transcription 3 activation and signaling, Endocrinology 150 (2009) 1122–1131.

[72] J. Yang, G.R. Stark, Roles of unphosphorylated STATs in signaling, Cell Res. 18 (2008) 443–451.
[73] O. Yermolaieva, N. Brot, H. Weissbach, S.H. Heinemann, T. Hoshi, Reactive oxygen species and nitric oxide mediate plasticity of neuronal calcium signaling, Proc. Natl. Acad. Sci. USA 97 (2000) 448–453.
[74] H. Yu, D. Pardoll, R. Jove, STATs in cancer inflammation and immunity: a leading role for STAT3, Nat. Rev. Cancer 9 (2009) 798–809.
[75] J.Y. Zheng, J. Sun, C.M. Ji, L. Shen, Z.J. Chen, P. Xie, Y.Z. Sun, R.T. Yu, Selective deletion of apolipoprotein E in astrocytes ameliorates the spatial learning and memory deficits in Alzheimer's disease (APP/PS1) mice by inhibiting TGF-beta/Smad2/STAT3 signaling, Neurobiol. Aging 54 (2017) 112–132.
[76] Z. Zhong, Z. Wen, J.E. Darnell Jr., Stat3: a STAT family member activated by tyrosine phosphorylation in response to epidermal growth factor and interleukin-6, Science 264 (1994) 95–98.